Cell, Vol. 90, 207–216, July 25, 1997, Copyright ©1997 by Cell Press

Microtubule Interaction Site of the Kinesin Motor

Günther Woehlke, Aaron K. Ruby, Cynthia L. Hart, Bernice Ly, Nora Hom-Booher, and Ronald D. Vale*
Howard Hughes Medical Institute
Departments of Pharmacology and Biochemistry
University of California, San Francisco
San Francisco, California 94143

Summary

Kinesin and myosin are motor proteins that share a common structural core and bind to microtubules and actin filaments, respectively. While the actomyosin interface has been well studied, the location of the microtubule-binding site on kinesin has not been identified. Using alanine-scanning mutagenesis, we have found that microtubule-interacting kinesin residues are located in three loops that cluster in a patch on the motor surface. The critical residues are primarily positively charged, which is consistent with a primarily electrostatic interaction with the negatively charged tubulin molecule. The core of the microtubule-binding interface resides in a highly conserved loop and helix (L12/α5) that corresponds topologically to the major actin-binding domain of myosin. Thus, kinesin and myosin have developed distinct polymer-binding domains in a similar region with respect to their common catalytic cores.

Introduction

Many cellular force-generating processes are executed by kinesin motor proteins that use microtubules as a track for movement. Kinesin motors constitute a large and still-expanding protein superfamily that shares a similar ~350-amino-acid (aa) force-generating element (termed the motor domain) (Goldstein, 1993; Vale and Fletterick, 1997). At present, >80 members of the kinesin superfamily have been entered into sequence databases, and it seems likely that the mammalian genome may contain >30 genes encoding distinct kinesin motors. Kinesin motors are involved in numerous cell biological processes that include organelle transport, maintenance of endoplasmic reticulum and intermediate filament distributions, organization of spindle microtubules, chromosome segregation, flagellar growth, and positioning of developmental morphogens (Bloom and Endow, 1995).

Kinesin motors have served as important model systems to study the mechanism of protein-based movement. The enzymatic cycle has been dissected by kinetic measurements (Hackney, 1994; Gilbert et al., 1995; Ma and Taylor, 1995, 1997), and the motility of individual kinesin motor proteins can be assayed in vitro by microscopic techniques. Prior motility studies have demonstrated that conventional kinesin (the first identified member of the kinesin superfamily) is a processive motor that can move along >100 tubulin subunits before dissociating from the microtubule (Howard et al., 1989; Block et al., 1990; Hackney, 1994; Vale et al., 1996). High resolution analyses of this movement using an optical trap microscope have shown that kinesin moves in 8 nm increments, which corresponds to the spacing between α/β tubulin subunits on the microtubule protofilament (Svoboda et al., 1993). Furthermore, the small size of the kinesin motor domain (which is less than one-half the size of myosin's motor domain) and the ability to express active motor in bacteria (Yang et al., 1990) have made kinesin an attractive system for structural studies.

The recent crystal structures of the motor domains of kinesin (Kull et al., 1996) and the kinesin-related protein Ncd (Sablin et al., 1996) revealed an unexpected structural similarity with the catalytic core of the actin-based motor myosin. The nucleotide-binding pockets of these motors also show many similarities with the corresponding region of G proteins, a group of "molecular switches" that exhibit nucleotide-dependent binding interactions with a variety of target proteins (Sablin et al., 1996; Smith and Rayment, 1996). The common features in the nucleotide pocket have provided further insight into how these proteins hydrolyze nucleotides and undergo nucleotide-dependent conformational changes (Vale, 1996). Thus, it seems likely that kinesin and myosin and possibly G proteins evolved from a common ancestral protein.

While the similarities between motors and G proteins have provided clues as to which elements of kinesin alter conformation during the enzymatic cycle, the precise structural changes that give rise to motility are still unknown. Moreover, the force-generating process must involve an intimate partnership between the motor and the filament. For example, microtubules stimulate the ATPase activity of kinesin by ~1000-fold, and microtubule binding is also undoubtedly required to elicit the correct conformational changes in the motor domain that give rise to forward movement. The interaction of kinesin motors with microtubules has been visualized at 20–30 Å resolution by cryo-electron microscopy (cryo-EM) (reviewed in Amos and Hirose, 1997). However, in contrast to the well-studied actin–myosin interface (dos Remedios and Moens, 1995), relatively little is known about the sites on kinesin that contact microtubules. However, deletion analysis of the motor domain indicates that the N-terminal 130 residues of the motor domain are not essential for microtubule binding (Yang et al., 1989).

In this study, we have identified microtubule-interacting residues of kinesin using alanine-scanning mutagenesis, an approach that has been used successfully to identify critical residues in various protein–protein interfaces (Wells, 1996). Here, we show that mutations in solvent-exposed residues that alter microtubule affinity reside primarily in three loops that cluster together in a patch. Alanine mutations of eight basic and two hydrophobic residues reduce microtubule affinity, while mutations of six acidic residues increase microtubule

*To whom correspondence should be addressed.

affinity, which is consistent with a strong ionic interaction of kinesin with acidic residues on tubulin. The most pronounced mutants are found in a loop that corresponds topologically to the major actin-binding domain located in the lower jaw (lower 50 kDa domain) of myosin.

Results

Preparation and Analysis of Kinesin Mutants

The kinesin motor domain has two principle faces that are divided by a central β sheet. One face contains the entrance to the nucleotide pocket and is comprised primarily of residues at the N terminus of the motor domain. It is unlikely that this face is involved in microtubule binding, since Yang et al. (1989) showed that deletion of the N-terminal 130 aa does not eliminate microtubule binding. For these reasons, we concentrated our mutagenesis efforts on the side of the motor domain opposite to the nucleotide-binding pocket. Using the crystal structure of the kinesin motor domain as a guide, 36 solvent-exposed residues (primarily charged or large hydrophobic; see Experimental Procedures) were selected for mutagenesis to alanine, since such mutations have been shown to have little or no effect on the energetics of protein folding (Matthews, 1996). The only region of ambiguity is L11, which is not visible in the kinesin crystal structure. However, several of the mutated L11 residues are highly conserved and correspond to solvent-exposed residues in Ncd.

Analyses of motor domain mutations were performed in a human kinesin aa 1–560 bacterial construct containing a C-terminal polyhistidine tag (K560). This bacterially expressed kinesin, which contains the motor domain and half of the α-helical coiled-coil stalk, exhibits processive movement along microtubules (Vale et al., 1996), which is similar to native kinesin (Howard et al., 1989; Block et al., 1990).

ATPase activity was selected as a screening method for analyzing mutant kinesin–microtubule interactions, since we found that it was more sensitive and more reproducible than direct microtubule-binding assays. Microtubules activate kinesin ATPase activity by ~1000-fold, and the microtubule dependence of the ATPase stimulation fits a Michaelis-Menten curve (Gilbert and Johnson, 1993) (Figure 1). The slow step in the enzymatic cycle in the absence of microtubules is ADP release (Hackney, 1988), and hence binding of kinesin-ADP to microtubules is required to promote nucleotide release and enhance the turnover rate of the motor. Therefore, the apparent Michaelis-Menten constant for microtubule-dependent ATPase activation (K_mMT) reflects an affinity between the kinesin motor and its microtubule substrate (see discussion of this parameter in the Experimental Procedures). The maximal ATP turnover rate (k_{cat}) and microtubule gliding speed in a motility assay, on the other hand, are determined by rate-limiting steps in the enzymatic cycle. Hence, mutations that alter microtubule-binding affinity, and not the rate constants of the enzymatic cycle, would be expected to exhibit an increased K_mMT but have a normal k_{cat} and microtubule gliding speed. An example of such a mutant (K240A) is shown in Figure 1.

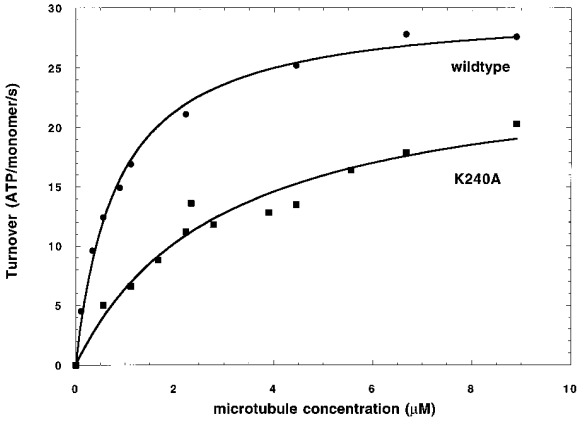

Figure 1. Microtubule-Stimulated ATPase Activity of Wild-Type and a Mutant Kinesin Protein, K240A

Activation of kinesin ATPase activity by microtubules was used to analyze alanine point mutants shown in Table 1. Maximal turnover (k_{cat}) and apparent Michaelis-Menten values (K_mMT) were determined from the best fit to a hyperbolic curve. In this representative example, the k_{cat} and K_mMT of wild-type and K240A were 30 ATP/head · s and 25 ATP/head · s, and 0.8 μM and 3.0 μM, respectively.

Mutations That Affect ATPase and Motor Activity

The ATPase measurements of wild-type K560 motor (94 assays performed on 26 independent protein preparations) yielded an average K_mMT of 1.1 ± 0.35 μM and a k_{cat} of 27 ± 7 ATP/s/motor domain. All mutant kinesin motors were purified and assayed in parallel with a wild-type motor as a control, and between two and four preparations of each mutant were analyzed. Results from the mutant kinesin motor proteins are presented in Table 1.

The majority of mutations showed little or no change in the K_mMT for microtubule-activated ATPase activity (gray residues in Figure 2A). Nine mutants (K141A, K159A, K240A, L248A, K252A, K256A, Y274A, K281A, and R284A) (yellow residues in Figure 2A), however, had 1.8- to 5-fold elevated K_mMT compared with wild-type kinesin (this lower threshold was selected as it corresponds to a value that is 2σ above the mean of the 94 wild-type K560 assays). One mutant (R278A) showed a >10-fold increase in K_mMT (red in Figure 2A). All of these mutants showed normal or close-to-normal microtubule gliding velocity, suggesting that these mutations did not significantly alter protein conformation or denature the molecule.

The mutations that increase K_mMT derive from the following regions of the kinesin structure: K141 and K159 belong to the L7/L8 region; K240, L248, and K252 are part of L11; K256 is part of α4; Y274 and R278 are part of L12; and K281 and R284 belong to α5 (Figure 2B). Although these residues are separated from one another in the primary sequence, they cluster in a similar region on the protein surface. In fact, K141, Y274, R278, K281, and R284 form a continuous, ~25 Å strip in the center of the protein, and residues K240, K252, and K256 are near this region (Figure 2A). Two mutants, L248A and K159A, are located above and below this central strip, respectively. Remarkably, eight of the ten K_mMT mutants are basic residues, and these residues contribute to a patch of electropositive charge that exists on this face

Table 1. Characterization of Single-Alanine Substitutions of Kinesin Surface Residues

	MT-Stimulated ATPase		MT Gliding	
Residue	K_mMT (fold wt)	K_{cat} (fold wt)	Velocity (fold wt)	Conservation
R278	15.5 ± 5.45	0.66 ± 0.30	0.76 ± 0.05	Superfamily
K252	4.37 ± 0.11	0.37 ± 0.07	1.07 ± 0.11	KHC
K240	4.22 ± 1.05	0.98 ± 0.01	0.62 ± 0.02	Superfamily
Y274	3.18 ± 0.42	0.75 ± 0.10	0.85 ± 0.10	Superfamily
L248	3.12 ± 0.94	0.75 ± 0.15	1.09 ± 0.03	Superfamily
K256	2.94 ± 0.78	0.71 ± 0.05	0.98 ± 0.47	Superfamily
K281	2.40 ± 0.99	0.88 ± 0.14	0.82 ± 0.15	Superfamily
K159	2.25 ± 0.21	1.02 ± 0.40	0.79 ± 0.09	KHC
R284	2.24 ± 0.54	0.43 ± 0.01	0.89 ± 0.10	N-term
K141	1.82 ± 0.01	1.06 ± 0.01	0.95 ± 0.01	KHC
H156	1.62 ± 0.43	1.12 ± 0.02	0.84 ± 0.12	KHC
K166	1.61 ± 0.39	1.01 ± 0.05	1.04 ± 0.26	KHC
Y164	1.43 ± 0.14	0.40 ± 0.04	0.88 ± 0.11	Superfamily
R161	1.18 ± 0.15	0.67 ± 0.01	0.88 ± 0.04	None
H129	1.11 ± 0.23	0.93 ± 0.08	0.99 ± 0.16	KHC
L153	1.09 ± 0.41	0.63 ± 0.06	0.96 ± 0.03	N-term
N263	1.07 ± 0.38	1.08 ± 0.16	1.07 ± 0.15	KHC
F172	1.03 ± 0.27	0.76 ± 0.12	1.06 ± 0.11	KHC
L139	1.02 ± 0.32	1.00 ± 0.07	1.04 ± 0.20	None
Q287	1.01 ± 0.28	0.89 ± 0.11	0.86 ± 0.03	N-term
E157	0.98 ± 0.08	0.43 ± 0.13	0.74 ± 0.02	N-term
P276	0.95 ± 0.01	0.93 ± 0.06	0.93 ± 0.02	Superfamily
Y138	0.88 ± 0.20	0.35 ± 0.04	0.22 ± 0.06	Superfamily
D147	0.85 ± 0.03	1.21 ± 0.84	1.02 ± 0.12	None
L317	0.84 ± 0.11	0.76 ± 0.01	1.14 ± 0.05	None
D249	0.81 ± 0.17	1.46 ± 0.54	0.60 ± 0.09	KHC
E220	0.62 ± 0.08	1.16 ± 0.50	1.13 ± 0.05	None
L223	0.72 ± 0.01	0.72 ± 0.02	0.95 ± 0.03	KHC
N152	0.65 ± 0.16	0.80 ± 0.08	0.86 ± 0.05	KHC
T273	0.60 ± 0.07	1.19 ± 0.33	0.96 ± 0.06	None
E250	0.54 ± 0.09	0.77 ± 0.14	0.56 ± 0.03	Superfamily
E270	0.47 ± 0.07	1.07 ± 0.03	1.07 ± 0.12	N-term
D279	0.44 ± 0.21	0.78 ± 0.14	0.83 ± 0.30	N-term
E170	0.39 ± 0.24	0.81 ± 0.27	0.64 ± 0.06	N-term
E311	0.32 ± 0.01	0.34 ± 0.06	0.31 ± 0.13	Superfamily
D140	0.29 ± 0.04	0.59 ± 0.08	0.55 ± 0.06	Superfamily

For explanation of the mutagenesis stragegy, see Experimental Procedures. Kinesin MT-stimulated ATPase (see Figure 1) and gliding velocities were measured on two to five independent batches of protein. the standard deviations indicate variability of different protein preparations. Relative values were calculated by comparison of mutant kinesins with a wild-type protein expressed, prepared, and assayed in parallel. Wild-type kinesin values for K_mMT and k_{cat} were generally consistent between preparations; the mean and standard deviations were 1.1 ± 0.35 mM and 27 ± 7 ATP/s/head, respectively. Microtubule gliding velocities varied among preparations but were very consistent for proteins prepared at the same time. Values between preparations ranged from 0.4–0.65 μm/s. The level of conservation of a residue is classified in four categories: "Superfamily", generally conserved throughout the entire kinesin superfamily (N-terminal, C-terminal, and internal domain motors) (Vale and Fletterick, 1997); "N-term", conserved among several or all five classes of N-terminal motors (conventional kinesins, monomeric motors [e.g., KIF1A], heterotrimeric motors [e.g., KRP 85/95], bimC family, and chromokinesins) (Hirokawa, 1996); "KHC", conserved among conventional kinesins only; "None", not conserved.

of the motor domain, as determined by surface potential analysis of the molecular surface using the program GRASP (not shown). Table 1 also shows that the majority of mutations that elevate K_mMT are in well-conserved residues.

Six mutants, D140A, E170A, E250A, E270A, D279A, and E311A (colored blue in Figure 2A), demonstrated a lower (<0.6-fold) K_mMT than wild-type kinesin. Interestingly, these negatively charged residues are highly conserved, and the majority are adjacent to positively charged residues that, when mutated to alanine, result in a higher K_mMT. It has been previously observed that alanine mutations of residues located in the center of a binding interface can produce a higher binding affinity (Cunningham and Wells, 1989). E170, however, is somewhat recesssed and more distantly removed from the other residues that affect K_mMT. It is unclear whether this residue is part of the binding interface or whether the effect of this alanine mutation is indirect.

Of the 36 single-alanine mutations examined, only four mutations (Y138A and D140A in L7, E250A in L11, and E311A in α6) significantly decreased the microtubule gliding velocity (by 2- to 4-fold) (Table 1). These residues are universally conserved in the kinesin superfamily and might be part of the activation pathway by which microtubules stimulate the kinesin ATPase activity. Three of these alanine mutations were also noted above as ones that exhibit a lower K_mMT. As discussed in the Experimental Procedures, a lower K_mMT could potentially result from a decrease in k_{cat} without a change in the equilibrium binding affinity of the motor for the microtubule.

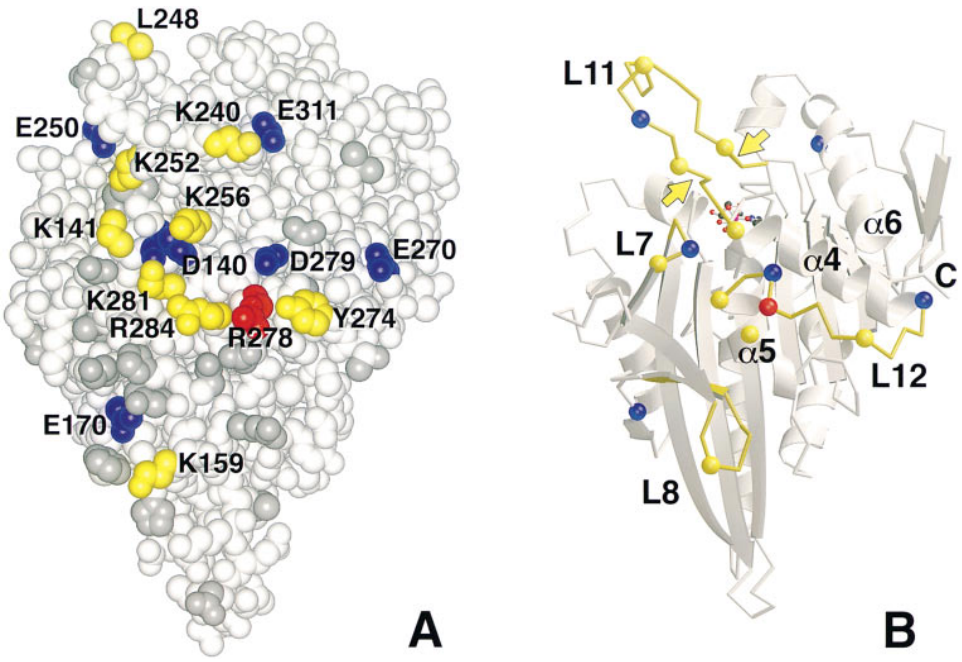

Figure 2. Location of Residues Targeted for Alanine Mutagenesis

(A) shows a space-filling model of the kinesin motor domain oriented with the nucleotide-binding pocket located on the back side. The effects of single-alanine substitutions are indicated according to the following coloring scheme: gray, wild-type behavior (0.6 to 1.8-fold relative K_mMT); yellow, 1.8 to 5-fold higher K_mMT; and red, >5-fold higher K_mMT. Blue indicates a decrease of K_mMT (<0.6-fold K_mMT). (B) shows a ribbon diagram of the motor in the same orientation, with balls indicating the positions of the affected residues shown as in (A). The positions of loops described in the text are highlighted in yellow. The arrows mark the region of loop 11 that is not visible in the crystal structure. The locations of the three α-helices on this face and the C terminus (aa 323) of the motor domain are also indicated. The configuration of the displayed intervening region is modeled based upon the Ncd L11 structure, whose position is visible in electron density maps.

Analysis of Triple Mutants

The results from the single-mutant analyses indicate that L7/L8, L11, and L12/α5 contain residues that contribute to the binding affinity of kinesin for microtubules. To investigate the relative contributions of these regions further, we prepared triple-alanine substitutions in nearby residues in L8 (E157A/K159A/Y164A), the tip of L11 (L248A/D249A/E250A), and L12/α5 (Y274A/R278A/K281A [named L12/α5–1] as well as Y274A/R278A/R284A [L12/α5–2]) (Figure 2). All three triple mutants demonstrated basal ATPase activity in the absence of microtubules (Table 2), indicating that they have a functional active site. These results suggest that the triple mutants are folded correctly.

The K_mMT for the L8 triple mutant was ~3-fold elevated over wild type, which was only slightly greater than the single-K159A mutation; the microtubule gliding velocity was only slightly reduced compared to wild type. The L11 triple mutant demonstrated a normal K_mMT, which may be due to the fact that mutations of L248 and E250 have opposing effects on K_mMT (Table 1). However, the L11 triple mutant exhibited a 4-fold reduction in microtubule gliding velocity and k_{cat}, suggesting that these conserved residues at the tip of L11 may be important for microtubule activation of the enzyme activity. While both L8 and L11 triple mutations produced active motors, the two L12/α5 triple mutants displayed neither measurable microtubule-stimulated ATPase activity nor microtubule gliding activity (Table 2). In the microtubule gliding assay, the L12/α5 triple mutants bound very few microtubules to the glass surface (even at very high kinesin surface densities), suggesting that many L12/α5 mutant proteins are required to attach simultaneously to a microtubule in order to hold it to the surface. Collectively, these results suggest that L12/α5 constitutes an essential microtubule-interacting region of the kinesin molecule.

Reduced Microtubule Binding of L12/α5 Triple Mutants

The defects of L12/α5 triple mutants described above could be due to a failure to bind to microtubules or to a defect of the bound microtubule to activate the motor ATPase activity. To address this question, we incubated kinesin with increasing concentrations of microtubules and measured the amount of bound kinesin by microtubule cosedimentation (Figure 3). Since the two heads of dimeric kinesin may exhibit complex binding to microtubules (Rosenfeld et al., 1996), microtubule cosedimentation experiments were performed using a monomeric kinesin construct that was employed previously for crystallographic studies (K349). With 1 mM MgADP, wild-type K349 bound to microtubules with a K_d of ~3 μM. In the presence of the ATP analog AMPPNP (1 mM) or the absence of nucleotide, kinesin is in a stronger microtubule-binding state, and >90% of the motor cosediments with 1 μM microtubules (indicating a K_d of <100 nM, which is consistent with other studies [Crevel et al., 1996]).

The L11 triple mutant in K349 exhibited very similar

Table 2. Characteristics of Kinesin Triple Mutations

Mutant	Basal ATPase (fold wt)	MT-Stimulated ATPase		MT Gliding
		KmMT (fold wt)	Kcat (fold wt)	Velocity (fold wt)
L8 (E157A, K159A, Y164A)	4.30 ± 0.71	3.35 ± 0.21	0.42 ± 0.01	0.78 ± 0.07
L11 (L248A, D249A, E250A)	1.07 ± 0.96	0.97 ± 0.36	0.21 ± 0.04	0.27 ± 0.05
L12/α5-1 (Y274A, R278A, K281A)	0.70 ± 0.13	UD	UD	UD
L12/α5–2 (Y274A, R278A, R284A)	0.68 ± 0.01	UD	UD	UD

Clusters of three nearby residues were exchanged to alanine, and the triple mutants analyzed for MT-stimulated ATPase and motility as described in Table 1 (standard deviations are shown for two independent protein preparations). Both loop L12/α5 triple mutants showed neither detectable MT-stimulated ATPase activity nor motility (UD, Undetectable). The basal ATPase activity for wild-type kinesin was 0.020 ± 0.005 (n = 8). Basal ATPase activity in the absence of microtubules was observed for all mutants, indicating that they are functional enzymes.

binding to wild-type kinesin under all nucleotide conditions (data not shown). In contrast, the L12/α5 triple mutants showed dramatically reduced microtubule binding in all nucleotide states compared to wild-type kinesin. In the presence of 1 mM ADP and AMPPNP (Figure 3), the L12/α5–2 triple mutant showed very low levels of binding, even at the highest microtubule concentrations used. Similar results were obtained with 1 mM ATP, and the L12/α5–1 mutant yielded identical results to L12/α5–2 (data not shown). The L12/α5–2 triple mutant exhibited some residual binding activity in the nucleotide-free state, although the affinity is still at least 50-fold lower than wild-type kinesin (Figure 3). Thus, the results from the microtubule cosedimention experiments indicate that L12/α5 is a critical microtubule-binding region of the kinesin motor domain.

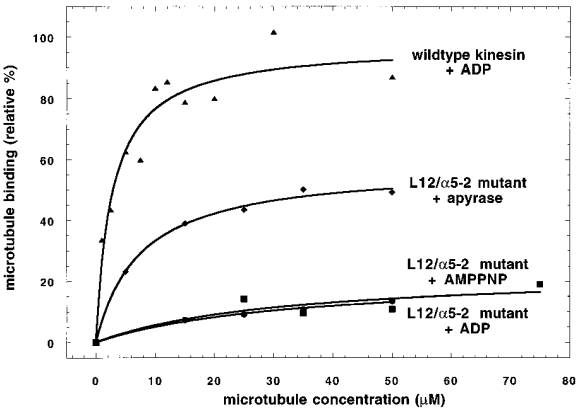

Figure 3. Binding Affinities of Wild-Type and L12/α5 Triple-Mutant Kinesin

The microtubule-binding affinity of the L12/α5–2 triple-mutant kinesin (monomeric k349) was compared to wild type using microtubule cosedimentation experiments. Three nucleotide conditions were tested in order to simulate different kinetic intermediate states. In the presence of ADP, the wild-type protein showed an apparent dissociation constant $K_d \approx 3$ μM (triangles), whereas the affinities in the presence of AMPPNP (presumably reflecting the ATP intermediate) and apyrase (nucleotide-free state) were too low to be measured (more than 90% kinesin bound with 1 μM microtubules). The L12/α5–2 triple mutant shows dramatically reduced binding affinities under all conditions. Only the strong nucleotide-free binding state retains significant affinity to microtubules (Kd ≈ 7 μM [diamonds]). In the presence of ADP as well as AMPPNP (circles and rectangles, respectively), the binding activity is very low and a K_d could not be measured. This agrees with microscopic observations where, in comparison to wild type, the number of microtubules adsorbed to the L12/α5 mutant kinesin-coated surface was greatly reduced in the presence of ATP and AMPPNP.

Discussion

Microtubule-Interacting Sites on the Kinesin Motor

Using alanine-scanning mutagenesis, we have identified a group of microtubule-interacting residues that cluster together on the kinesin motor domain. This represents a comprehensive mutagenesis study of a motor–polymer-binding interface. The mutant proteins were characterized by a functional assay involving microtubule stimulation of the ATPase activity. While indirect, this assay is expected to reflect the direct binding of the motor to the microtubule, and motor–microtubule cosedimentation experiments are consistent with this interpretation.

The changes in microtubule affinity that we have observed are most likely a consequence of the side chain substitutions rather than more global changes in protein structure. First, the mutated residues are solvent-exposed, and the side chains do not form hydrogen bonds with the polypeptide chain in the atomic model. More significantly, only four of the 36 single-mutant kinesin proteins have significantly lower microtubule gliding velocities, indicating that the motor function of the majority of mutant proteins is normal or close to normal. The triple L12/α5 mutants, which have drastically reduced microtubule binding, are also likely to be folded correctly, since they display basal ATPase activity that is similar to the wild-type motor.

This mutagenesis study suggests that the kinesin–tubulin-binding interface is dominated by ionic interactions. This result is consistent with studies demonstrating that the association of kinesin with microtubules decreases dramatically with increasing salt concentration (Gilbert et al., 1995; Ma and Taylor, 1995; Vale et al., 1996). Remarkably, eight of the ten mutations that result in a lower microtubule affinity are in positively charged residues. It is attractive to speculate that some of these positively charged residues on the kinesin surface form interactions with a group of glutamic acid

residues at the C terminus of tubulin. Consistent with this idea, a recent study shows that the C terminus of tubulin plays an important role in kinesin binding (Tucker and Goldstein, 1997). Interestingly, we also find that several acidic residues at the microtubule-binding interface may decrease the affinity of kinesin for microtubules. Alanine-scanning studies of other protein–protein interfaces have also uncovered mutants that increase binding affinity (Cunningham and Wells, 1989). It should also be mentioned that we cannot exclude residues other than the 16 described in this study as participating in the interface. For example, Pearce et al. (1996) showed that residues that form van der Waals contacts in protein–protein interfaces as defined by crystallographic studies sometimes do not produce significant changes in binding affinity when mutated to alanine. Conversely, some of the 16 residues may not contact tubulin directly and mutation effect may be indirect.

The residues that we have identified as influencing kinesin's interaction with microtubules are all conserved among the conventional kinesin motors. Moreover, 13 of the 16 mutations are conserved either within several kinesin classes that have N-terminal motor domains or within the entire superfamily. These findings suggest that the microtubule interface is conserved among kinesin motors, which is consistent with cryo-EM studies showing that kinesin and Ncd bind in the same orientation and approximately same position on the microtubule (Hirose et al., 1995; Arnal et al., 1996). However, differences in the binding interface may also exist between subfamilies of related kinesin motors. For example, kinesin R284, a mutation which decreases microtubule affinity, is a conserved basic residue in all kinesins whose motor domain is at the N terminus of the polypeptide chain, but is a conserved hydrophobic residue in C-terminal motors such as Ncd (R. Case and R. D. V., unpublished data). It is unclear whether such subtle chemical differences could account for the different directions of movement of kinesin and Ncd along microtubules (McDonald et al., 1990; Walker et al., 1990). Interestingly, the monomeric motors such as KIF1A/B (Nangaku et al., 1994; Okada et al., 1995) are distinctive in having an insertion containing several lysine residues in L12. This extra positive charge may increase the affinity of these motors for microtubules. Myosin motors also contain a class-specific, actin-binding loop (termed loop 2; Spudich, 1994; Uyeda et al., 1994; Mooseker and Cheney, 1995) that contains variable numbers of lysine residues. Thus, although the microtubule interface appears to be well conserved overall, class-specific variations appear to exist that may influence the performance of different classes of kinesin motors.

The mutagenesis studies suggest that several regions of the kinesin motor contribute residues to the tubulin-binding interface (primarily L7/L8, L11, and L12/α5). Although L11 is not defined by present crystallographic data, the distance from the residues at the tip of L11 to L8 is probably 15–20 Å. An extensive contact with the microtubule is also suggested by cryo-EM studies of kinesin motor–microtubule complexes (reviewed in Amos and Hirose, 1997). Moreover, docking of the atomic structure onto three-dimensional reconstructions of cryo-EM images of Ncd bound to microtubules are in good agreement with the functional mutagenesis studies described here (see discussion in the accompanying paper, Sosa et al., 1997 [this issue of *Cell*]). While the contact area of the microtubule may be extensive, our findings indicate that L12/α5 constitutes a "hot spot" that contributes the majority of the binding free energy. Supporting this idea, the single-alanine mutation with the greatest effect on K_mMT (R278A) maps to this region. Even more significantly, triple mutants of residues in L12/α5 produce dramatic decreases in microtubule-binding affinity. L12/α5 also contains the most highly conserved cluster of solvent-exposed residues in the kinesin superfamily.

Comparison of Kinesin's Microtubule-Binding Interface with Structurally Related Proteins

Crystallographic studies revealed that kinesin and myosin share a common structural fold, and it was speculated that the filament-binding interface of these two motors may be positioned similarly in their three-dimensional structures (Kull et al., 1996). The present data is consistent with this hypothesis. The core microtubule-binding loop of kinesin (L12) between α4 and α5 corresponds topologically in myosin to a large insertion of $\sim$140 aa located between two equivalent helices (Figure 4). Biochemical and structural data indicates that this insertion, which forms the lower 50 kDa domain ("lower jaw") of the myosin motor, contains several elements that together contribute a large portion of the actin-binding interface (Rayment et al., 1993a, 1993b). Functional studies suggest that loop 2 (which precedes a helix equivalent to α5 in kinesin) forms an initial contact with actin that is necessary for stimulating phosphate release and governs the velocity of actin transport (Spudich, 1994). A second actin-binding region of myosin is a loop in the upper 50 kDa domain that contains a critical arginine (R403 in human β cardiac myosin) that is frequently mutated in patients with familial hypertrophic cardiomyopathies. This loop is part of a large domain that corresponds topologically to the smaller L7/L8 loops of kinesin motors, which our studies indicate also play some role in microtubule binding. Thus, two microtubule-binding loops of kinesin, L12 and L7/L8, are substituted by much larger domains in myosins that also are involved in polymer binding. These results indicate that these two motors have distinct polymer-binding interfaces that are in similar positions with reference to their shared structural core.

The third region that we, as well as Sosa et al. (1997), have identified as interacting with microtubules (L11/α4) has a structural counterpart not only in myosin, but in G proteins as well. The active sites of motors and G proteins contain two loops, termed switch I and switch II, that are believed to interact with the γ-phosphate when ATP is in the pocket and then change conformation when the γ-phosphate is released (Vale, 1996). The switch II loop and subsequent helix in G proteins and myosin change their conformations in NTP and NDP states, and therefore the homologous regions in kinesin (L11/α4) are likely to undergo nucleotide-dependent changes as well. The switch II loop and helix in myosin are largely buried and hence are unlikely to interact with

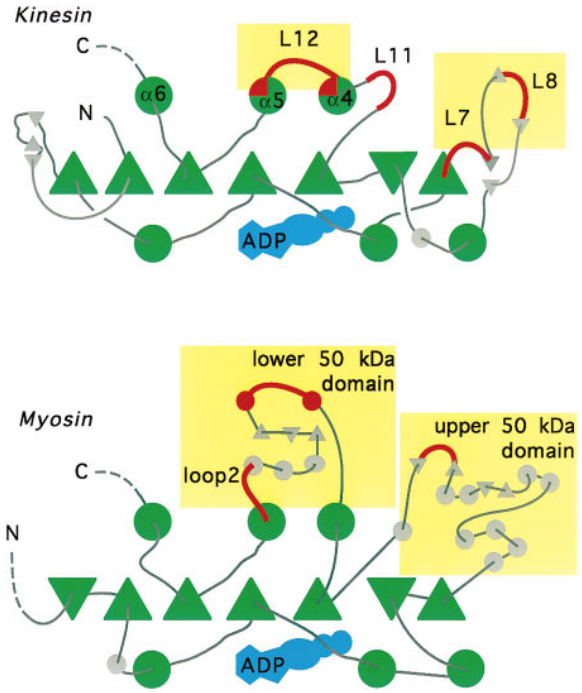

Figure 4. Comparison of the Polymer-Binding Regions of Kinesin and Myosin

Triangles represent β-strands and circles are helices; the orientation of the structural elements is indicated by the direction of the triangles and the emergence of loops from the circles and triangles. Secondary structural elements shown in green represent ones that superimpose in the kinesin and myosin structures (Kull et al., 1996). The smaller gray elements are ones that are unique in the two motors. Regions marked in red bind to the filament, as evidenced by decreased binding affinity (higher K_mMT) of kinesin mutants and structural and biochemical studies on myosin. The yellow boxes highlight the 50 kDa subdomains in myosin and their counterparts in kinesin. See Discussion for further details.

actin directly. In contrast, the switch II loop and helix have been shown to participate directly in the interface of G proteins and their targets (e.g., transducin-α with the βγ complex [Wall et al., 1995; Lambright et al., 1996] and EfTu with EfTs [Kawashima et al., 1996]).

Coordination between the Nucleotide-Binding Site and the Microtubule Interface

The binding affinity of kinesin for microtubules changes during the nucleotide cycle; in the absence of nucleotide and in the presence of ATP, the binding affinity is high and in the presence of ADP, the interaction is weakened (Romberg and Vale, 1993; Gilbert et al., 1995; Ma and Taylor, 1995). Hence, information from the nucleotide active site must be relayed to the microtubule-binding site to change its conformation and alter its affinity. The microtubule-interacting loops described in this study are located nearby and could receive information from these switch regions. L7 is located in close proximity to switch I, and the N terminus of L11 contains the γ-phosphate-interacting residues of switch II. L12 is also connected at its N terminus to the α4 helix, and the comparable helices in myosin and G proteins undergo significant nucleotide-dependent conformational changes (Milburn et al., 1990; Fisher et al., 1995). The increase in binding affinity from the ADP to ATP state could involve repositioning of residues or the recruitment of new residues to the binding interface; further work with the mutants identified in this study may help to address this question. The connection between the switch regions and structures involved in microtubule binding is also suggested by the locations of several mutants in Drosophila Ncd (β6) (Moore et al., 1996) and S. cerevisiae Kar3 (α4) (Hoyt et al., 1993) that were identified by genetic screens.

Microtubule binding to kinesin must also induce a conformational change in the nucleotide-binding site that causes a 10-fold acceleration of the hydrolytic step (Ma and Taylor, 1995) and a >1000-fold acceleration of the rate of ADP release (Hackney, 1988). Our study has identified four mutations (Y138A, D140A, E250A, and E311A) that have both a lower k_{cat} and a slower microtubule gliding velocity than wild-type kinesin and therefore appear to be defective in activation of the mechanochemical cycle. These residues are highly conserved throughout the kinesin superfamily and are located in positions that were speculated to be functionally important (Kull et al., 1996; Sablin et al., 1996). Y138 and D140 are both very close to switch I. E250 is found at the tip of L11 (the switch II loop), which is thought to contact the groove between two microtubule protofilaments (see Sosa et al., 1997). E311 is the only conserved, solvent-exposed residue in α6, a structural element that is thought to be important for mechanical amplification. These conserved residues may be part of the microtubule-activation pathway, and the steps in the enzymatic cycle that are affected by these mutations are being further characterized.

Experimental Procedures

Cloning and Mutagenesis

Kinesin and kinesin mutants were expressed as bacterial recombinant proteins comprising amino acid residues 1–560 with a C-terminal five-histidine tag (HLHHHH). The leucine in the histidine tag was introduced by an oligonucleotide error, but the construct was retained, since proteins with this tag purified comparably to His(x6) tag proteins on Ni-NTA columns (Qiagen Inc.). Hydrodynamic studies show that this K560 protein forms stable dimers as well as a small amount of tetramers (Pierce et al., personal communication). The histidine-tagged K560 coding sequence was cloned into the NdeI/XhoI site of the IPTG-inducible pET17b plasmid (Novagene Inc.).

Site-specific mutagenesis was initially performed using techniques based on M13-phage ssDNA (Amersham Sculptor Kit) and later by Stratagene's QuikChange protocol (Stratagene Inc.). However, the QuikChange protocol (Stratagene Inc.) proved to be more efficient for introducing mutations and was used for preparing the later mutations in this study. For mutagenesis, a 1.2 kb XbaI-HindIII fragment of the expression vector (comprising the translation initiation elements and coding sequence for aa 1–389) was subcloned into pBluescript SK(+), and ssDNA was obtained using standard procedures (Sambrook et al., 1989). Oligonucleotides were designed that introduced the desired alanine-point mutation(s) along with a silent mutation, which introduced a restriction site that could be used to screen colonies for correctly mutagenized plasmids. A 0.7 kb NcoI-SacI fragment coding for aa 122–365 of the kinesin motor domain was sequenced and cloned back into the pET17b expression vector.

Residues selected for this study were qualitatively judged to be solvent-exposed in the crystal structure. For an initial mapping of

the microtubule-binding site, a set of 19 point mutations (residues 129, 139, 147, 156, 159, 161, 164, 166, 172, 220, 223, 248, 250, 256, 270, 274, 279, 284, and 317) was generated, with the amino acid substitutions evenly distributed over the kinesin motor domain opposite to the nucleotide-binding site. For further definition of the interaction site with microtubules, a second series of 13 mutants (140, 141, 152, 153, 157, 240, 249, 252, 263, 273, 278, 281, and 287) was created, introducing alanine mutations at locations where effects had been observed or results had been ambiguous. A final set of four mutants (Y138, E170, P276, and E311) was generated to complete the series. Of the charged and large hydrophobic residues on this face of the kinesin, approximately six residues (E127, K131, K150, D158, K213, and K222) were not examined in this alanine scan. In the context of another ongoing study, several mutations have been made in L2 (P45D, A47D, and K44Q/P45T/A47R), and all showed no significant change ($<$50%) in K_mMT, k_{cat}, and gliding velocity.

Expression and Purification of Kinesin Proteins

Freshly transformed E. coli BL21 cells were grown at 22°C from a single colony in 1.0 l of media (20 g/l tryptone, 15 g/l yeast extract, 8 g/l NaCl, 10 mM glucose, 2 g/l Na_2HPO_4, 1 g/l KH_2PO_4, and 50 μg/ml ampicillin). Expression was induced with 0.1 mM IPTG at cell densities between $OD_{600} \approx 0.5$–1.0, and the cells were harvested 14 to 18 hr later.

Kinesin was partially purified (30%–50%, depending on the expression level) in a single step by Ni^{2+}-affinity chromatography (Ni-NTA-resin, Qiagen, Inc.). Typically, four or five mutant proteins were prepared in parallel with a wild-type protein as a control. The bacterial cells were resuspended in buffer A (50 mM Na-phosphate buffer [pH 8], 1 mM $MgCl_2$, 250 mM NaCl, and 1 mM Pefabloc [Boehringer Mannheim]) and were disrupted in a French press at 0.8 MPa (18,000 psi). Insoluble material was removed by centrifugation for 35 min at 27,000 × g. Supernatants were incubated on a roller at 4°C for 1 hr with 1 ml of Ni^{2+} resin and transferred into a column. The columns were washed with buffer A containing 60 mM imidazole (pH 6) until absorbance at 280 nm was below 0.1. Kinesin was eluted with 0.25 M imidazole (pH 6) in buffer A supplemented with 50 μM ATP and stored in elution buffer with 20% (w/v) sucrose in small aliquots in liquid nitrogen. Control experiments with bacteria containing only the vector without insert showed that no background ATPase activity was copurified. Protein concentrations were determined by analyzing CCD images of Coomassie-stained SDS-polyacrylamide gels. A BSA-standard curve was run on the same gel along with the kinesin, and protein concentrations were calculated using optical densities quantified with the computer program NIH image. Typical 1 l kinesin K560 preparations yielded 1.5 mg of protein at 0.5–1.0 mg/ml.

For binding assays, a monomeric kinesin construct was used (K349, aa 1–349). Purification of wild-type and loop 11 triple mutants was accomplished on a cellulose phosphate column and a MonoQ column as described (Kull et al., 1996). As L12/α5 triple mutants did not bind to cellulose phosphate, an alterate protocol was used. For these preparations, the bacterial wild-type and mutant cell pellets were resuspended in 25 mM imidazole · HCl buffer (pH 6.8), 1 mM $MgCl_2$, 1 mM EGTA, and 50 mM NaCl, and were disrupted by a French press at 0.8 MPa. The extract was loaded onto a 25 ml DEAE-sepharose fast-flow column and fractionated with a NaCl gradient (0.05–1 M). Kinesin eluted around 250 mM. The peak fractions were combined, diluted to 50 mM NaCl with 25 mM Pipes · NaOH (pH 6.8), 1 mM $MgCl_2$, and 1 mM EGTA, and were loaded on a MonoQ column. A 0.05–1 M NaCl gradient in Pipes buffer eluted kinesin at 300 mM NaCl. This protocol yielded a protein preparation with two contaminating bands of high molecular weight. Proteins were stored in liquid nitrogen after addition of 2 μM ATP and 10% (w/v) sucrose.

Microtubule-Stimulated ATPase

MT-stimulated ATPase activity of kinesin was assayed in a coupled enzymatic assay (Huang and Hackney, 1993). Tubulin was purified using published protocols (Hyman et al., 1990). For each day of assays, a tubulin aliquot was thawed, prespun (Beckman TLA ultracentrifuge, 10 min at 380,000 × g), and then polymerized in the presence of 1 mM GTP and 20 μM paclitaxel at 37°C. Microtubules were purified and concentrated by an additional centrifugation step over 40% sucrose in BRB80 (80 mM Pipes [pH 6.8], 1 mM EGTA, and 1 mM $MgCl_2$) and then resuspended in the desired buffer (see below) containing 20 μM paclitaxel. Tubulin concentration was calculated from absorbance at 280 nm in 6 M guanidine, using an extinction coefficient of 1.03 ml/mg/cm and M_r = 100,000 for the tubulin dimer.

The ATPase assays (Huang and Hackney, 1993) were performed in 12 mM Pipes · NaOH (pH 6.8), 2 mM $MgCl_2$, 1 mM EGTA (ATPase buffer) containing 0.5 mM ATP and a coupled NADH oxidation system (1.5 mM KCl, 0.2 mM NADH, 0.5 mM phospho(enol)pyruvate, 0.01 U of pyruvate kinase, and 0.03 U lactate dehydrogenase). Microtubules were added to 0–8 μM concentration. At higher concentrations, scattering effects rendered the readings unreliable. The assays were started with 100–200 nM kinesin, and extinction at 340 nm was recorded. Control experiments showed the assay was approximately linear with kinesin concentration. The Michaelis-Menten constant for ATP was ~50 μM for wild-type kinesin, which is in agreement with published values. The K_mMT and k_{cat} values were determined using a hyperbolic curve-fitting routine in the program Kaleidagraph. Due to errors of the fit and determination of motor protein concentration, the values of k_{cat} are less accurate than K_mMT. An assessment of both k_{cat} and microtubule gliding velocity is valuable in determining whether a mutation has a defect in turnover.

Interpretation of ATPase Data

The apparent K_mMT reflects an affinity of kinesin for the microtubule, its allosteric activator. Since the enzyme transits through multiple intermediate states in its catalytic cycle, the affinity as measured by K_mMT reflects the collection of the equilibrium dissociation constants (K_d) of the various transient states in the cycle. Ignoring any complications associated with cooperativity between kinesin's two heads, the kinesin cycle can be illustrated by the scheme below:

$$\begin{array}{ccccccccc} & & 1 & & 2 & & 3 & & 4 \\ \text{MT-K}+\text{T} & \rightleftharpoons & \text{MT-K-T} & \rightarrow & \text{MT-K-DP} & \rightarrow & \text{MT-K-D} & \rightleftharpoons & \text{MT-K} \\ & & \Updownarrow K_d(\phi) & & \Updownarrow K_d(\text{T}) & & \Updownarrow K_d(\text{DP}) & & \Updownarrow K_d(\text{D}) \\ \text{K} + \text{T} & \rightleftharpoons & \text{K-T} & \rightarrow & \text{K-DP} & \rightarrow & \text{K-D} & & \end{array}$$

where MT: microtubules, K: kinesin, D, T, P: ADP, ATP, HPO_4^{2-}, respectively, and $K_d(\phi)$, K_d(T), K_d(DP), and K_d(D): dissociation constants in the nucleotide-free, ATP, ADP-P, and ADP states.

Previous kinetic studies have provided information on how K_mMT may be related to kinesin's affinity for microtubules (reviewed in Hackney, 1996). First, pre-steady-state measurements indicate that steps two (hydrolysis) and three (phosphate release) are effectively irreversible, and the rate of dissociation of kinesin from the microtubule is very small in the MT-K, MT-K-T, and MT-K-DP states compared to the weaker binding MT-K-D state (Ma and Taylor, 1997). As a result, kinesin proceeds through steps one through three while remaining bound to the microtubule. Therefore, microtubule dissociation and rebinding procedes primarily through the K-D state. Since the ADP dissociation rate is 1000-fold slower in the absence of microtubules, the K-D complex can also be considered to be a dead-end intermediate that can only reenter the reaction cycle by binding to a microtubule. With these arguments, K_mMT is related both to the equilibrium binding constant of K-D for microtubules [K_d(D)] and to the relative amount of kinesin molecules that populates the MT-K-D intermediate state (k_{cat}/k4, with k4 representing the first-order rate constant for ADP release), as follows: $K_m\text{MT} = (k_{cat}/k4) \cdot K_d(\text{D})$. If dissociation of MT-K-DP contributes to the reaction, as suggested by some models (Gilbert et al., 1995), then the relationship of K_m to dissociation constants is more complex, but it is still an approximate of measure of equilibrium binding.

These considerations suggest that mutants that display a shifted K_mMT but otherwise unaffected k_{cat} most likely reflect microtubule-binding changes primarily in the ADP state. Also, if k_{cat} and microtubule gliding velocity do not change noticably, it is unlikely that the rate-limiting ADP-release step is attenuated. In cases where the k_{cat} changes significantly (for example in D140A, E170A, E250A, and E311A, which have both reduced K_mMT and k_{cat}/gliding velocity), the relationship between K_mMT and microtubule affinity requires

additional information on which transitions in the enzymatic cycle are affected.

Basal ATPase Activity

MT-independent basal ATPase activity was assayed using a malachite green phosphate assay (Geladopoulos et al., 1991). Kinesin was exchanged into ATPase buffer on a Sephadex G25 desalting column (Pharmacia NAP-10 columns). The reaction of duplicate samples was initiated at room temperature by addition of 1 mM ATP, and four 20 μl aliquots were taken over 30 min.

Motility Assay

A motility assay in which microtubules glide over kinesin-coated surfaces was used to assess the motor function of mutant proteins. A 10 μl mixture of BRB80 containing 2 mM $MgCl_2$ containing kinesin, rhodamine-labeled microtubules (~20 μg/ml) (Hyman et al., 1990), an oxygen depletion system (71.5 mM β-mercaptoethanol, 22.5 mM glucose, 0.22 mg/ml glucose oxidase [Sigma G-2133], 0.036 mg/ml catalase [Sigma C-40]), and 1.5 mg/ml casein was prepared and introduced into a flow chamber consisting of a glass slide and coverslip separated by adhesive tape.

The kinesin concentration used was generally ~5 μg/ml, although for weak microtubule-binding mutants (e.g., R278A), higher concentrations of motor were required to observe binding and motility. Gliding microtubules were visualized by fluorescence microscopy, and the image was recorded onto video tape using a SIT camera. Velocities were measured using a computer-based program.

Kinesin Binding to Microtubules

To assess microtubule binding of mutant kinesin motors, cosedimentation assays were perfomed with a monomeric motor construct comprising aa 1–349 (Kull et al., 1996). Microtubules were prepared as for ATPase assays, and binding was measured in a final volume of 120 μl ATPase buffer, complemented with 1 mM nucleotide · $MgCl_2$ or 2 U/ml apyrase, respectively. Binding was initiated by addition of kinesin (0.1–0.3 μM), and after 10 min, free and MT-bound fractions were separated by centrifugation (10 min for 380,000 × g in a Beckman TLA ultracentrifuge). Equal amounts of unspun samples and MT pellets were compared on quantitative SDS gels as described above. Recovery was checked by comparison of supernatants and pellets.

Computer Analyses

Space-filling models of kinesin were generated on a Silicon Graphics (SGI) workstation using Insight II (Biosym Inc.), and ribbon diagrams were generated with MolScript (Kraulis, 1991) and rendered using Raster3D (Meritt and Murphy, 1994). Figures were then edited in Adobe Photoshop.

Acknowledgments

We thank Roger Cooke, Robert Fletterick, Brinda Govindan, and Laura Romberg for comments on the manuscript. We are also especially grateful to Ed Taylor for his insight into the interpretation of the ATPase data and Jon Kull and Robert Fletterick for assistance in preparing figures. Virginia Cooke also provided valuable help in analyzing microtubule gliding velocity. A. R. and R. D. V. were supported by a NIH program project grant AR42895, and G. W. was supported by the Deutsche Forschungsgemeinschaft and the Swiss National Foundation.

Received April 11, 1997; revised June 13, 1997.

References

Amos, L.A., and Hirose, K. (1997). The structure of microtubule-motor complexes. Curr. Opin. Cell Biol. *9*, 4–11.

Arnal, I., Metoz, F., DeBonis, S., and Wade, R.H. (1996). Three-dimensional structure of functional motor proteins on microtubules. Curr. Biol. *6*, 1265–1270.

Block, S.M., Goldstein, L.S., and Schnapp, B.J. (1990). Bead movement by single kinesin molecules with optical tweezers. Nature *348*, 348–352.

Bloom, G., and Endow, S. (1995). Motor proteins 1: kinesin. Protein Profile *1*, 1112–1138.

Crevel, I.M.-T.C., Lockhart, A., and Cross, R.A. (1996). Weak and strong states of kinesin and ncd. J. Mol. Biol. *257*, 66–76.

Cunningham, B.C., and Wells, J.A. (1989). High-resolution epitope mapping of the hGH-receptor interactions by alanine-scanning mutagenesis. Science *244*, 1081–1085.

dos Remedios, C.G., and Moens, P.D. (1995). Actin and the actomyosin interface: a review. Biochim. Biophys. Acta *1228*, 99–124.

Fisher, A.J., Smith, C.A., Thoden, J.B., Smith, R., Sutoh, K., Holden, H.M., and Rayment, I. (1995). X-ray structures of the myosin motor domain of Dictyostelium discoideum complexed with MgADP.BeFx and MgADP.AlF4-. Biochemistry *34*, 8960–8972.

Geladopoulos, T.P., Sotiroudis, T.G., and Evangelopoulos, A.E. (1991). A malachite green colorimetric assay for protein phosphatase activity. Anal. Biochem. *192*, 112–116.

Gilbert, S.P., and Johnson, K.A. (1993). Expression, purification, and characterization of the Drosophila kinesin motor domain produced in Escherichia coli. Biochemistry *32*, 4677–4684.

Gilbert, S.P., Webb, M.R., Brune, M., and Johnson, K.A. (1995). Pathway of processive ATP hydrolysis by kinesin. Nature *373*, 671–676.

Goldstein, L.S. (1993). With apologies to Scheherazade: tails of 1001 kinesin motors. Annu. Rev. Genet. *27*, 319–351.

Hackney, D.D. (1988). Kinesin ATPase: rate-limiting ADP release. Proc. Natl. Acad. Sci. USA *85*, 6314–6318.

Hackney, D.D. (1994). Evidence for alternating head catalysis by kinesin during microtubule-stimulated ATP hydrolysis. Proc. Natl. Acad. Sci. USA *91*, 6865–6869.

Hackney, D.D. (1996). The kinetic cycles of myosin, kinesin, and dynein. Annu. Rev. Physiol. *58*, 731–750.

Hirokawa, N. (1996). Organelle transport along microtubules-the role of KIFs. Trends Cell Biol. *6*, 135–141.

Hirose, K., Lockhart, A., Cross, R.A., and Amos, L.A. (1995). Nucleotide-dependent angular change in kinesin motor domain bound to tubulin. Nature *376*, 277–279.

Howard, J., Hudspeth, A.J., and Vale, R.D. (1989). Movement of microtubules by single kinesin molecules. Nature *342*, 154–158.

Hoyt, M.A., He, L., Totis, L., and Saunders, W.S. (1993). Loss of function of Saccharomyces cerevisiae kinesin-related cin8 and kip1 is suppressed by KAR3 motor domain mutations. Genetics *135*, 35–44.

Huang, T.-G., and Hackney, D.D. (1993). Drosophila kinesin minimal motor domain expressed in Escherichia coli: purification and kinetic characterization. J. Biol. Chem. *269*, 16493–16501.

Hyman, A., Dreschel, D., Kellogg, D., Salser, S., Sawin, K., Steffen, P., Wordeman, L., and Mitchison, T. (1990). Preparation of modified tubulins. Meth. Enzymol. *196*, 303–319.

Kawashima, T., Berthet-Colominas, C., Wulff, M., Cusack, S., and Leberman, R. (1996). The structure of the Escherichia coli EF-Tu-EF-Ts complex at 2.5 Å resolution. Nature *379*, 511–518.

Kraulis, P.J. (1991). MOLSCRIPT: a program to produce both detailed and schematic plots of protein structures. J. Appl. Cryst. *24*, 946–950.

Kull, F.J., Sablin, E.P., Lau, R., Fletterick, R.J., and Vale, R.D. (1996). Crystal structure of the kinesin motor domain reveals a structural similarity to myosin. Nature *380*, 550–555.

Lambright, D.G., Sondek, J., Bohm, A., Skiba, N.K., Hamm, H.E., and Sigler, P.B. (1996). The 2.0 Å crystal structure of a heterotrimeric G protein. Nature *379*, 311–319.

Ma, Y.Z., and Taylor, E.W. (1995). Mechanism of microtubule kinesin ATPase. Biochemistry *34*, 13242–13251.

Ma, Y.Z., and Taylor, E.W. (1997). Interacting head mechanism of microtubule-kinesin ATPase. J. Biol. Chem. *272*, 724–730.

Matthews, B.W. (1996). Structural and genetic analysis of the folding and function of T4 lysozyme. FASEB J. *10*, 35–41.

McDonald, H.B., Stewart, R.J., and Goldstein, L.S. (1990). The kinesin-like ncd protein of Drosophila is a minus end-directed microtubule motor. Cell *63*, 1159–1165.

Meritt, E.A., and Murphy, M.E.P. (1994). Raster3D version 2.0: a program for photorealistic molecular graphics. Acta Cryst. *D50*, 869–873.

Milburn, M.V., Tong, L., deVos, A.M., Brunger, A., Yamaizumi, Z., Nishimura, S., Kim, S.-H. (1990). Molecular switch for signal transduction: structural differences between active and inactive forms of protooncogenic ras proteins. Science *247*, 939–945.

Moore, J.D., Song, H., and Endow, S.A. (1996). A point mutation in the microtubule binding region of the Ncd motor protein reduces motor velocity. EMBO J. *15*, 3306–3314.

Mooseker, M.S., and Cheney, R.E. (1995). Unconventional myosin. Annu. Rev. Cell Biol. *11*, 633–675.

Nangaku, M., Sato-Yoshitake, R., Okada, Y., Noda, Y., Takemura, R., Yamazaki, H., and Hirokawa, N. (1994). KIF1B, a novel microtubule plus end-directed monomeric motor protein for transport of mitochondria. Cell *79*, 1209–1220.

Okada, Y., Yamazaki, H., Sekine-Aizawa, Y., and Hirokawa, N. (1995). The neuron-specific kinesin superfamily protein KIF1A is a unique monomeric motor for anterograde axonal transport of synaptic vesicle precursors. Cell *81*, 769–780.

Pearce, K.H., Ultsch, M.H., Kelley, R.F., de Vos, A.M., and Wells, J.A. (1996). Structural and mutational analysis of affinity-inert contact residues at the growth hormone-receptor interface. Biochemistry *35*, 10300–10307.

Rayment, I., Holden, H.M., Whittaker, M., Yohn, C.B., Lorenz, M., Holmes, K.C., and Milligan, R.A. (1993a). Structure of the actin-myosin complex and its implications for muscle contraction. Science *261*, 58–65.

Rayment, I., Rypniewski, W., Schmidt-Base, K., Smith, R., Tomchick, D., Benning, M.M., Winkelmann, D.A., Wesenberg, G., and Holden, H.M. (1993b). The three-dimensional structure of myosin subfragment-1: a molecular motor. Science *261*, 50–58.

Romberg, L., and Vale, R.D. (1993). Chemomechanical cycle of kinesin differs from that of myosin. Nature *361*, 168–170.

Rosenfeld, S.S., Rener, B., Correia, J.J., Mayo, M.S., and Cheung, H.C. (1996). Equilibrium studies of kinesin-nucleotide intermediates. J. Biol. Chem. *271*, 9473–9482.

Sablin, E.P., Kull, F.J., Cooke, R., Vale, R.D., and Fletterick, R.J. (1996). Crystal structure of the motor domain of the kinesin-related motor ncd. Nature *380*, 555–559.

Sambrook, J., Fritsch, E.F., and Maniatis, T. (1989). Molecular Cloning: A Laboratory Manual, 2nd Ed. (Cold Spring Harbor: Cold Spring Harbor Laboratory Press).

Smith, C.A., and Rayment, I. (1996). Active site comparisons highlight structural similarities between myosin and other P-loop proteins. Biophys. J. *70*, 1590–1602.

Sosa, H., Dias, P., Hoenger, A., Whittaker, M., Wilson-Kubalek, E., Sablin, E., Fletterick, R.J., Vale, R.D., and Milligan, R.A. (1997). A model for the microtubule-ncd motor protein complex obtained by cryo-electron microscopy and image analysis. Cell, this issue, *90*, 217–224.

Spudich, J.A. (1994). How molecular motors work. Nature *372*, 515–518.

Svoboda, K., Schmidt, C.F., Schnapp, B.J., and Block, S.M. (1993). Direct observation of kinesin stepping by optical trapping interferometry. Nature *365*, 721–727.

Tucker, C., and Goldstein, L.S.B. (1997). Probing the kinesin-microtubule interaction. J. Biol. Chem. *272*, 9481–9488.

Uyeda, T.Q., Ruppel, K.M., and Spudich, J.A. (1994). Enzymatic activities correlate with chimaeric substitutions at the actin-binding face of myosin. Nature *368*, 567–569.

Vale, R.D. (1996). Switches, latches, and amplifiers: common themes of molecular motors and G proteins. J. Cell Biol. *135*, 291–302.

Vale, R.D., and Fletterick, R.J. (1997) The design plan of kinesin motors. Annu. Rev. Cell Biol., in press.

Vale, R.D., Funatsu, T., Pierce, D.W., Romberg, L., Harada, Y., and Yanagida, T. (1996). Direct observation of single kinesin molecules moving along microtubules. Nature *380*, 451–453.

Walker, R.A., Salmon, E.D., and Endow, S.A. (1990). The Drosophila claret segregation protein is a minus-end directed motor molecule. Nature *347*, 780–782.

Wall, M.A., Coleman, D.E., Lee, E., Iniguez-Lluhl, J.A., Posner, B.A., Gilman, A.G., and Sprang, S.R. (1995). The structure of the G protein heterotrimer. Cell *83*, 1047–1058.

Wells, J.A. (1996). Binding in the growth hormone receptor complex. Proc. Natl. Acad. Sci. USA *93*, 1–6.

Yang, J.T., Laymon, R.A., and Goldstein, L.S. (1989). A three-domain structure of kinesin heavy chain revealed by DNA sequence and microtubule binding analyses. Cell *56*, 879–889.

Yang, J.T., Saxton, W.M., Stewart, R.J., Raff, E.C., and Goldstein, L.S. (1990). Evidence that the head of kinesin is sufficient for force generation and motility in vitro. Science *249*, 42–47.